



ELSEVIER



CrossMark



# Low-Cost EM-Simulation-Driven Multi-Objective Optimization of Antennas

Adrian Bekasiewicz<sup>1\*</sup>, Slawomir Koziel<sup>2†</sup>, and Leifur Leifsson<sup>2‡</sup>

<sup>1</sup>*Gdansk University of Technology, Poland*

<sup>2</sup>*Reykjavik University, Iceland*

*adrian.bekasiewicz@eti.pg.gda.pl, koziel@ru.is, leifurth@ru.is*

## Abstract

A surrogate-based method for efficient multi-objective antenna optimization is presented. Our technique exploits response surface approximation (RSA) model constructed from sampled low-fidelity antenna model (here, obtained through coarse-discretization EM simulation). The RSA model enables fast determination of the best available trade-offs between conflicting design goals. A low-cost RSA model construction is possible through initial reduction of the design space. Optimization of the RSA model has been carried out using a multi-objective evolutionary algorithm (MOEA). Additional response correction techniques have been subsequently applied to improve selected designs at the high-fidelity EM antenna model level. The refined designs constitute the final Pareto set representation. The proposed approach has been validated using an ultra-wideband (UWB) monocone and a planar Yagi-Uda antenna.

*Keywords:* Antenna design, EM-driven design, surrogate-based optimization, multi-objective optimization

## 1 Introduction

Design and optimization of contemporary antennas is a challenging and multifaceted task. A realistic setup of modern antenna comprises not only the driven element with its feeding circuit but also connectors, housing and/or measurement fixtures. The only way to ensure accurate evaluation of a structure in such a configuration is through high-fidelity electromagnetic (EM) analysis. For reliability reasons, also the antenna design process has to be based on EM simulations. This is a time consuming process, which is usually carried out by means of computationally expensive, repetitive parameter sweeps.

Strict performance requirements for contemporary antennas create the necessity of simultaneous account for many (often conflicting) goals including not only the minimization of reflection

\* Faculty of Electronics, Telecommunications and Informatics

† Engineering Optimization & Modeling Center, School of Science and Engineering

‡ Engineering Optimization & Modeling Center, School of Science and Engineering

characteristics within the frequency band of interest, but also reduction of antenna footprint (Jungsuek and Sarabandi, 2013), minimization of side-lobe level (Sharaqa and Dib, 2013), cross polarization (Afshinmanesh, *et al.* 2008), or maximization of gain (Cao *et al.*, 2012), to name just a few. Simultaneous accounting for many objectives is significantly more challenging than single-objective optimization. In particular, if the designer priorities are not clearly defined, multi-objective optimization becomes a necessity (Kuwahara, 2005; Yang, *et al.* 2008). The aim of multi-objective optimization is to seek for trade-off solutions between non-commensurable goals forming a so-called Pareto optimal set (Deb, 2001). Only if the design preferences can be articulated a priori, the problem can be scalarized using, e.g., weighted sum or Chebyshev method (Deb, 2001). This is, however, an experience driven process which leads to different Pareto optimal-sets depending on a particular scalarization setup (Eichfelder, 2008).

One of the most popular approaches for generating a Pareto set is to utilize population-based metaheuristics with the emphasis on genetic algorithms (GA) (Koulouridis *et al.*, 2007; Ding and Wang, 2013) and particle swarm optimizers (PSO) (Jin and Rahmat-Samii, 2010; Afshinmanesh, *et al.* 2008). The most important advantage of these methods is the ability to process and outcome the entire set of solutions in a single simulation run. Nevertheless, this benefit comes at the expense of tremendous cost of thousands or even tens of thousands of objective evaluations (Kuwahara, 2005; Afshinmanesh, *et al.* 2008), which prohibits direct use of population-based metaheuristics together with EM simulators as evaluation tools, unless multi CPU resources provided by supercomputers or GPU-based simulations together with multiple CAD software licenses are available (Hannien, 2012).

The difficulty related to high computational cost of EM-simulation-driven optimization may be alleviated by incorporation of sensitivity data (Nair and Webb, 2003), however, fast determination of derivatives through adjoint sensitivity techniques is not yet widely available in commercial EM simulation tools. On the other hand, surrogate based optimization (SBO) techniques including manifold mapping (Koziel *et al.*, 2013), shape preserving response prediction (Koziel *et al.*, 2012), or space mapping (Bandler *et al.*, 2004), are very promising approaches for solving such expensive EM-driven design problems. In SBO, direct optimization of computationally expensive antenna model is replaced by an iterative correction and re-optimization of its less accurate, yet fast low-fidelity model. In case of antennas, the low-fidelity model is usually obtained from coarse-discretization EM simulations of the high-fidelity model of a structure of interest. SBO methods proved to be very efficient design tools capable of yielding desired solutions at the cost of a few simulations of high-fidelity antenna model. Moreover, the design cost may be further reduced by incorporation of response surface approximation (RSA) models together with SBO techniques. However, most of the SBO approaches have so far been applied in the context of single-objective antenna design (Koziel and Ogurtsov, 2011).

In case of multi-objective optimization, especially when the algorithms of choice are population-based metaheuristics, a direct use of EM simulation tools is prohibitive. A workaround might be to use RSA models that replace EM evaluations in the process of seeking for Pareto optimal set. Nonetheless, the cost of RSA model setup (specifically acquiring the training data) grows exponentially with a number of designable parameters, which becomes impractical for large design spaces or if large number of design variables is involved. In practice, feasible construction of RSA model is limited to problems with a few parameters.

In (Koziel and Ogurtsov, 2013), a surrogate-based multi-objective optimization method combining coarse-discretization EM simulations and RSA models has been proposed. The technique allows for finding a representation of a Pareto optimal set at a low computational cost, however with restriction of up to a few designable parameters. The dimensionality issue was partially addressed in (Koziel and Ogurtsov, 2013) by the use of structure decomposition. On the other hand, the applicability of the approach (Koziel and Ogurtsov, 2013) is limited because decomposition cannot be used for majority of antenna structures.

In this work, we discuss a simple technique for design space reduction that aims at extending the range of applicability of the approach presented in (Koziel and Ogurtsov, 2013). The proposed method is based on identifying extreme points of the Pareto optimal set obtained through separate single-objective optimizations of the antenna structure with respect to individual design goals of interest, one at a time. The reduced space is defined by the hypercube determined by these extreme nodes and it is considerably (by orders of magnitude volume-wise) smaller than the initial one. This allows for feasible construction of the RSA surrogate even for larger number of design variables. Our approach is illustrated using two examples: a 3-variable UWB monocone antenna optimized with respect to reflection and overall size and 8-variable planar Yagi-Uda antenna, where objectives are minimization of reflection and maximization of the antenna gain within the frequency band of interest.

## 2 Methodology

In this section, we describe the proposed multi-objective optimization procedure. In particular, we formulate the multi-objective antenna design problem and outline the optimization approach. The optimization algorithm is validated in Section 3 using two design examples.

### 2.1 Multi-objective antenna design problem

We denote by  $\mathbf{R}_f(\mathbf{x})$  a response vector of an accurate high-fidelity model of antenna under consideration.  $\mathbf{R}_f$  may represent an antenna reflection, gain, etc. A vector  $\mathbf{x}$  represents designable parameters, specifically, geometry dimensions.

Let  $F_k(\mathbf{x})$ ,  $k = 1, \dots, N_{obj}$ , be a  $k$ th design objective. A common objective is minimization of antenna reflection within a frequency band of interest; however some geometrical objectives, i.e., minimization of the antenna size defined in practically meaningful way (maximal lateral size, overall occupied area, or antenna volume) may be also of interest. Objectives related to gain, or radiation pattern may be defined in a similar way.

If  $N_{obj} > 1$  then any two designs  $\mathbf{x}^{(1)}$  and  $\mathbf{x}^{(2)}$  for which  $F_k(\mathbf{x}^{(1)}) < F_k(\mathbf{x}^{(2)})$  and  $F_l(\mathbf{x}^{(2)}) < F_l(\mathbf{x}^{(1)})$  for at least one pair  $k \neq l$ , are not commensurable, i.e., none is better than the other in the multi-objective sense. We define the Pareto dominance relation  $\prec$  (Deb, 2001) saying that for the two designs  $\mathbf{x}$  and  $\mathbf{y}$ , we have  $\mathbf{x} \prec \mathbf{y}$  ( $\mathbf{x}$  dominates  $\mathbf{y}$ ) if  $F_k(\mathbf{x}) < F_k(\mathbf{y})$  for all  $k = 1, \dots, N_{obj}$ . The goal of multi-objective optimization is to find a representation of a Pareto optimal set  $X_p$  of the design space  $X$ , such that for any  $\mathbf{x} \in X_p$ , there is no  $\mathbf{y} \in X$  for which  $\mathbf{y} \prec \mathbf{x}$  (Deb, 2001).

### 2.2 Optimization algorithm

The high-fidelity model  $\mathbf{R}_f$  is computationally too expensive to be directly optimized in a multi-objective sense. In order to speed up the design process, a fast coarse-mesh surrogate model  $\mathbf{R}_{cd}$  is utilized. The  $\mathbf{R}_{cd}$  model is usually 10 to 50 times faster than  $\mathbf{R}_f$ , which is still too expensive for efficient multi-objective optimization. Therefore, another auxiliary response surface approximation (RSA) model  $\mathbf{R}_s$  is prepared (here, using kriging interpolation (Simpson *et al.*, 2001)) with the training data set consisting of sampled  $\mathbf{R}_{cd}$  model data. We use Latin Hypercube Sampling (Beachkofski and Grandhi, 2002) as a design of experiments technique. The kriging model  $\mathbf{R}_s$  is very smooth, fast and easy to optimize. However, the cost of acquiring the training data may be very high, particularly if the design space dimension is large. In order to make the RSA model setup feasible, it is critically important to perform an initial design space reduction. The proposed reduction approach is explained in detail in Section 2.3.

The main optimization engine used to identify a set of Pareto optimal solution is a multi-objective evolutionary algorithm (MOEA) with fitness sharing, mating restrictions and Pareto dominance tournament selection (Deb, 2001). MOEA-optimized RSA model  $\mathbf{R}_s$  becomes the initial

approximation of the Pareto set. In the next step,  $K$  designs selected from that initial set, i.e.,  $\mathbf{x}_s^{(k)}$ ,  $k = 1, \dots, K$ , are refined using surrogate-based optimization to find a Pareto front representation at the high-fidelity EM model level. Without loss of generality, we consider here two design objectives  $F_1$  and  $F_2$ . The chosen  $\mathbf{x}_s^{(k)}$  solutions are refined using output space mapping (OSM) algorithm of the following form (Koziel *et al.*, 2008):

$$\mathbf{x}_f^{(k,i+1)} = \arg \min_{\mathbf{x}, F_2(\mathbf{x}) \leq F_2(\mathbf{x}_s^{(k,i)})} F_1(\mathbf{R}_s(\mathbf{x}) + [\mathbf{R}_f(\mathbf{x}_s^{(k,i)}) - \mathbf{R}_s(\mathbf{x}_s^{(k,i)})]) \quad (1)$$

The goal of design space refinement is to minimize  $F_1$  for each design  $\mathbf{x}_f^{(k)}$  without altering objective  $F_2$ . The correction of surrogate model  $\mathbf{R}_s$  using the OSM term  $\mathbf{R}_f(\mathbf{x}_s^{(k,i)}) - \mathbf{R}_s(\mathbf{x}_s^{(k,i)})$  (here,  $\mathbf{x}_f^{(k,0)} = \mathbf{x}_s^{(k)}$ ) ensures that it coincides with  $\mathbf{R}_f$  at the beginning of each iteration. Usually only 2 to 3 iterations of (1) are required to find desired high-fidelity model design  $\mathbf{x}_f^{(k)}$ . The OSM procedure is repeated for all  $K$  chosen samples, resulting in the Pareto set composed of refined high-fidelity solutions. The block diagram of the design flow is shown in Fig. 1.

It should be stressed out that the high-fidelity model  $\mathbf{R}_f$  is not evaluated until the design refinement stage. One should also emphasize that the cost of finding the Pareto optimal set composed of high-fidelity models is only about three evaluations of the high-fidelity model per design. The construction of a kriging interpolation model is performed using a DACE toolbox (Lophaven *et al.*, 2002). More detailed explanations of antenna optimization using MOEA can be found in (Koziel and Ogurtsov, 2013).

### 2.3 Design space reduction

In design problems related to modern antennas, the initial ranges for geometry parameters are usually rather wide to ensure that the optimum design (or, in case of multi-objective optimization, the Pareto optimal set) resides within the prescribed frontiers. Generation of the RSA model in such a large design space especially when multi-parameter designs are considered is virtually impractical. Therefore, the initial solution space reduction is crucial for successful RSA-driven antenna optimization.

The Pareto optimal set usually resides in a very small fraction of the initial design space. Moreover, in the context of multi-objective antenna optimization only fragment of the Pareto optimal set representing the designs with reflection coefficient  $|S_{11}| \leq -10$  dB within the frequency band of interest is considered important. The illustration example of the Pareto optimal set in the 3-dimensional solution space is shown in Fig. 2.

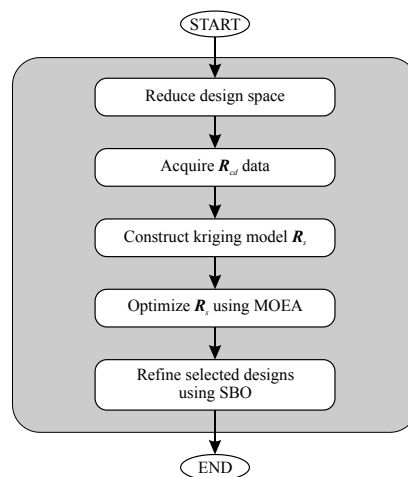


**Figure 1:** The design flow of the proposed algorithm.

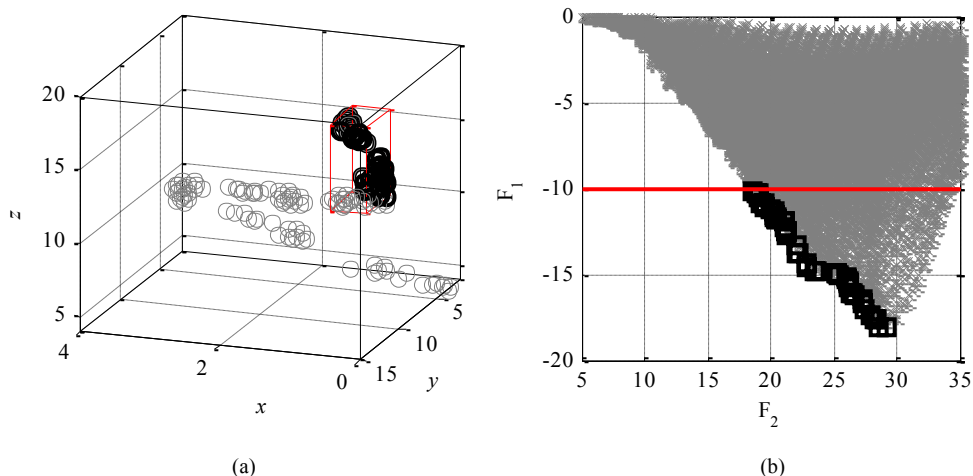


**Figure 2:** (a) Visualization of the Pareto optimal set (○) in 3-dimensional solution space. The portion of the design space that contains the part of the Pareto set we are interested in (red cuboid, where  $F_1 \leq -10$ ) is only a small fraction of the initial space. (b) the Pareto set of interest (□) versus the entire design space mapped to the feature space (×).

In the proposed approach, boundaries of the solution space are reduced using the following procedure. Let  $\mathbf{l}$  and  $\mathbf{u}$  be the initially defined lower/upper bounds for the design parameters. Consider

$$\mathbf{x}_{cd}^{*(k)} = \arg \min_{\mathbf{l} \leq \mathbf{x} \leq \mathbf{u}} F_k(\mathbf{R}_{cd}(\mathbf{x})) \tag{2}$$

where  $k = 1, \dots, N_{obj}$ , is considered as optimum design of the low-fidelity model obtained with respect to  $k$ th objective. Vectors  $\mathbf{x}_{cd}^{*(k)}$  determine the extreme points of the Pareto optimal set. The bounds of the reduced design space are then defined as (see Fig. 2 for conceptual illustration):  $\mathbf{l}^* = \min\{\mathbf{x}_{cd}^{*(1)}, \dots, \mathbf{x}_{cd}^{*(N_{obj})}\}$ ,  $\mathbf{u}^* = \max\{\mathbf{x}_{cd}^{*(1)}, \dots, \mathbf{x}_{cd}^{*(N_{obj})}\}$ .

In practice, the reduced design space is a very small fraction of the initial one, which makes the creation of the RSA model computationally feasible. One should note that no guarantee that the refined design space contains the entire Pareto optimal set being of interest is given, however, the majority of it is usually accounted for (together with the two aforementioned extreme points).

### 3 Case study

In this section, the proposed design space reduction for RSA-driven multi-objective optimization is demonstrated using two design examples: a 3-variable UWB monocone and an 8-variable narrow-band, planar Yagi-Uda antenna.

#### 3.1 UWB monocone antenna

Consider a UWB monocone antenna shown in Fig. 3(a). The structure is feed through a 50 Ω coaxial input (Teflon filling,  $r_0 = 0.635$  mm). Here, no extra circuitry is used for matching. The design specification imposed on the reflection response of the monocone is  $|S_{11}| \leq -10$  dB within 3.1 to 10.6 GHz. Design variables are  $\mathbf{x} = [z_1 \ z_2 \ r_1]^T$  (sizes in mm), where  $z_1$  is the extension of the coax pin,  $z_2$  is

the length of the cone section, and  $r_1$  is the size of the radial line section as shown in Fig. 3(b). The ground plane is modeled with infinite lateral extends.

Both the high-fidelity model of the antenna ( $\sim 1,000,000$  mesh cells, average evaluation time of 4 min), and the coarse-discretization model  $\mathbf{R}_{cd}$  ( $\sim 19,000$  mesh cells, average simulation time of 20 s) are simulated in CST Microwave Studio (CST, 2013). The design space is defined by  $0 \leq z_1 \leq 4$ ,  $2 \leq z_2 \leq 15$ ,  $4 \leq r_1 \leq 20$ , and a linear constraint  $z_1 + z_2 \leq r_1 - 0.25$ . The antenna size defined here is the maximal dimension out of vertical and lateral ones:  $A(\mathbf{x}) = \max\{2r_2, z_1 + z_2 + r_2\}$ , where  $r_2 = (r_1^2 - (z_1 + z_2)^2)^{1/2}$  is the radius of the hemisphere terminating the conical section. Two design objectives are considered: (i) minimization of  $|S_{11}|$  within the frequency band of interest (objective  $F_1(\mathbf{x})$ ) and (ii) reduction of the antenna size (objective  $F_2(\mathbf{x})$ ).

The initial solution space is defined by the following lower/upper bounds:  $\mathbf{l} = [0 \ 2 \ 4]^T$  and  $\mathbf{u} = [4 \ 15 \ 20]^T$ . A methodology from Section 2.3 is used for the determination of lower/upper bounds of the refined design space:  $\mathbf{l}^* = [0 \ 12.4 \ 14]^T$  and  $\mathbf{u}^* = [0.4 \ 13.2 \ 19.7]^T$ , resulting in reduction of the design space of interest by a factor of 456 (volume-wise). We utilized pattern search (Kolda *et al.*, 2003) as single-objective optimization engine.

The kriging interpolation model is created within the refined design space using only 50  $\mathbf{R}_{cd}$  samples obtained using Latin Hypercube Sampling. The average relative error of the  $\mathbf{R}_s$  model is only 3.5%. One should emphasize that the initial design space reduction is crucial for the generation of a reliable kriging model using such a small number of  $\mathbf{R}_{cd}$  samples. Average error of the model constructed using the same amount of 50  $\mathbf{R}_{cd}$  samples within initial design space is around 37% which is too high for the model to be used in the optimization process. The comparison of the model errors is shown in Fig. 4.

Subsequently, the initial Pareto optimal set has been found by optimizing the surrogate model using MOEA. Then, a set of 10 design samples selected from the initial Pareto set has been refined as described in Section 2.2. The results indicate that the minimum size of the considered antenna that still fulfills the requirements upon reflection is 19.8 mm, while the minimum reflection coefficient is  $-18.65$  dB (size is 28.3 mm). Moreover, the minimum size of the antenna, which satisfies requirements upon reflection, is over 30% smaller than the structure optimized with respect to  $|S_{11}|$ . Figure 5 shows the low-fidelity model solutions obtained within the refined design space and the Pareto sets of the low- and high-fidelity models.

The total optimization cost, including two single-objective optimizations (96 evaluations of the coarse-mesh  $\mathbf{R}_{cd}$  model), construction of the kriging interpolation model within the refined design space (50  $\mathbf{R}_{cd}$  evaluations), as well as the refinement step (30  $\mathbf{R}_f$  simulations) corresponds to only 41 evaluations of the high-fidelity model ( $\sim 3$  hours). The aggregated cost is negligible comparing to direct multi-objective optimizations, which needs around few thousands  $\mathbf{R}_f$  model evaluations (estimated on the basis of  $\mathbf{R}_s$  evaluations during MOEA optimization).

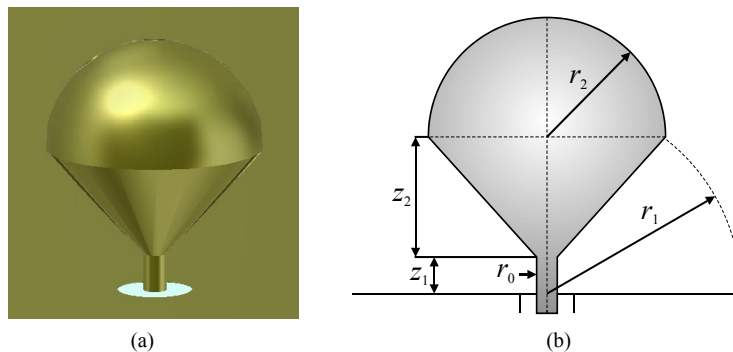
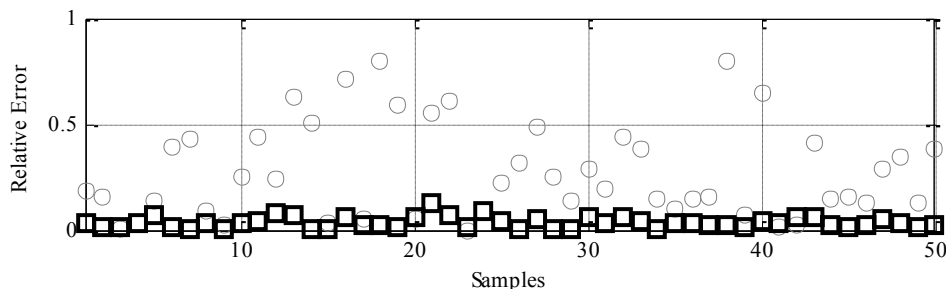
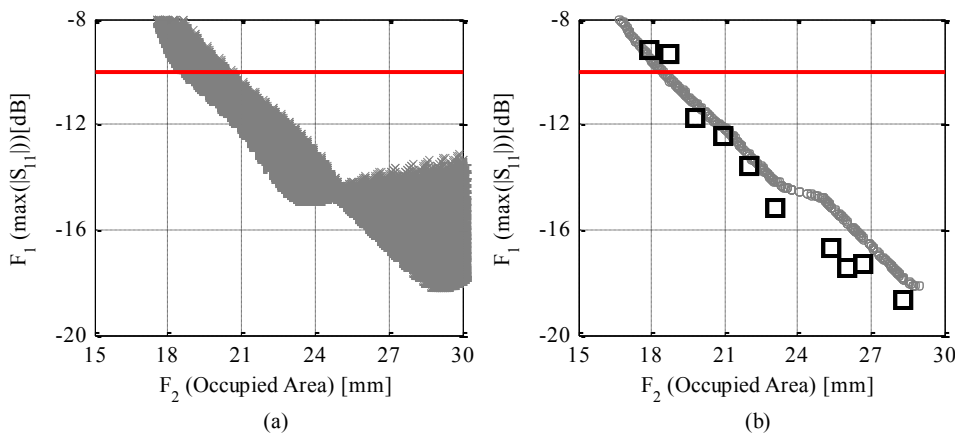


Figure 3: UWB monocone: (a) 3D view; (b) the cut view [20].



**Figure 4:** Relative error of a kriging interpolation model constructed using 50 LHS samples in the initial design space (○) and in the refined design space (□).



**Figure 5:** UWB monocone antenna: (a) solution space; (b) Pareto optimal set obtained for low- (○) and high-fidelity (□) model.

### 3.2 Planar Yagi-Uda antenna

The second example is a planar Yagi-Uda antenna shown in Fig. 6, which comprises a driven element fed by a microstrip-to-cps transition, a director and a balun (Qian *et al.*, 1998). The input impedance is 50 Ω. The substrate is Rogers RT6010 ( $\epsilon_r = 10.2$ ,  $\tan\delta = 0.0023$ ,  $h = 0.635$  mm). The antenna contains eight variables:  $\mathbf{x} = [s_1 s_2 v_1 v_2 u_1 u_2 u_3 u_4]^T$ . Parameters  $w_1 = 0.6$ ,  $w_2 = 1.2$ ,  $w_3 = 0.3$  and  $w_4 = 0.3$  remain fixed. The design objectives are to minimize the reflection coefficient and maximize the mean gain in the 10 to 11 GHz frequency range. Both the high-fidelity model  $\mathbf{R}_f$  and the coarse-mesh model  $\mathbf{R}_{cd}$  are simulated in CST Microwave Studio (CST, 2013) with evaluation time of 18 min (~1,512,000 mesh cells) and 110 s (~86,000 mesh cells), respectively. The initial lower/upper bounds are  $\mathbf{l} = [3.5 2.5 8 4 3 4.5 1.5 1]^T$ , and  $\mathbf{u} = [4.5 4.5 10 5.5 4.5 5.5 2.5 2]^T$ .

Design space reduction resulted in the refined lower/upper bounds of  $\mathbf{l}^* = [4.1 3.63 8.11 4.27 3.6 4.68 2.17 1.51]^T$ ,  $\mathbf{u}^* = [4.33 4.39 8.9 5.2 3.8 4.85 2.2 1.55]^T$ , which gives 6-orders smaller design space (volume-wise). The kriging interpolation model has been constructed using 300  $\mathbf{R}_{cd}$  samples. The average error of the model prepared in the refined design space is 0.1% for  $F_1$  and 4% for  $F_2$ , whereas the average error of the model generated in the initial solution space is 1% for  $F_1$  and 20% for  $F_2$ , making it unusable for multi-objective optimization. The comparison of the model errors is shown in Fig. 7.

15 samples selected from the initial Pareto optimal set were refined in only 2 iterations (per design) using the methodology of Section 2.2 (see Fig. 8). The obtained results indicate minimum antenna reflection of -18.3 dB (5.6 dB average in-band gain), and maximum 6.5 dB mean gain for -10 dB in-band reflection.

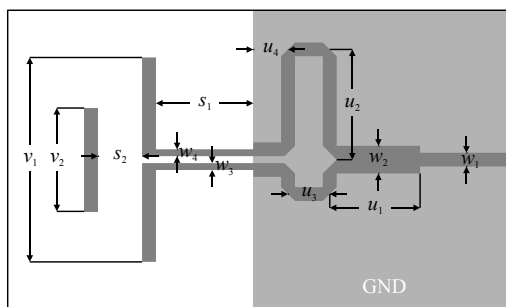


Figure 6: Geometry of eight-variable, planar Yagi-Uda antenna.

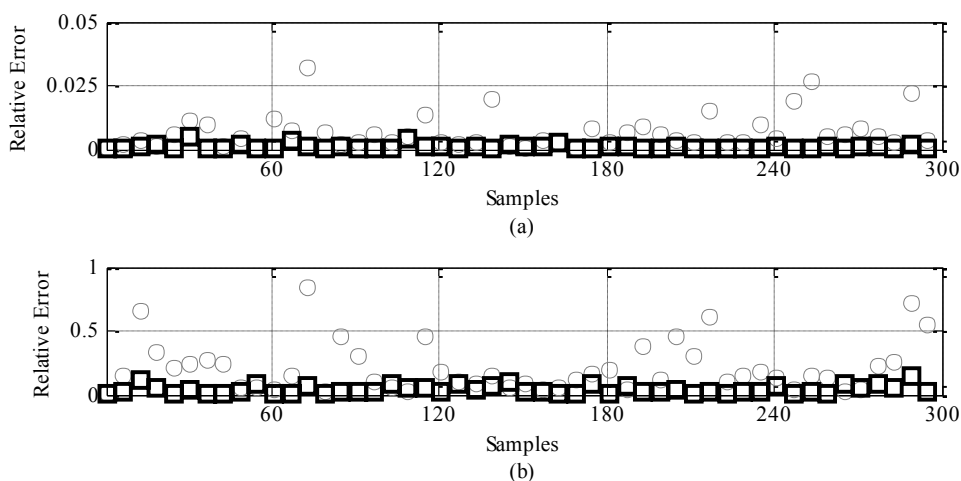


Figure 7: Relative error of the kriging interpolation model constructed using 300 LHS samples in the initial design space (○) and in the refined design space (□): (a) objective  $F_2$ ; (b) objective  $F_1$ .

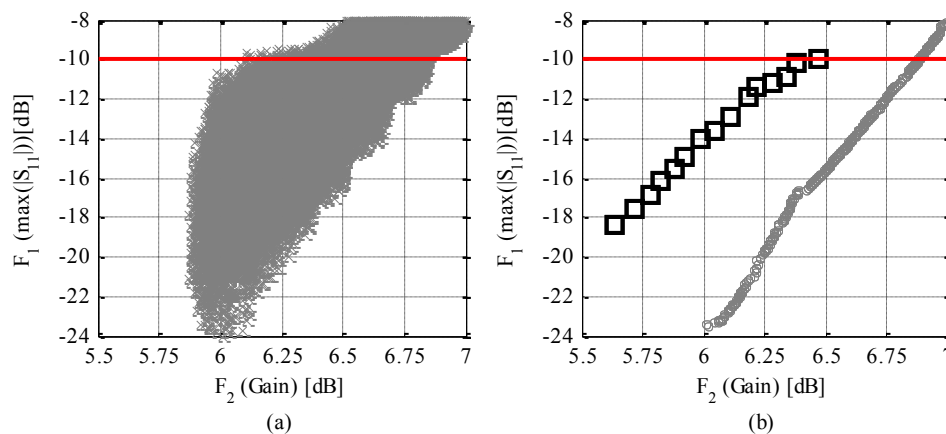


Figure 8: Planar Yagi-Uda antenna: (a) the entire design domain mapped to the feature space; (b) Pareto optimal set obtained for the low- (○) and the high-fidelity (□) model.



The overall computational cost of the optimization process, including the design space reduction (160  $R_{cd}$  evaluations), generation of 300  $R_{cd}$  samples for RSA model, and MOEA optimization, together with the refinement of the selected samples ( $\sim 34 R_f$  evaluations) corresponds to about 80 high-fidelity model simulations. The final optimization cost ( $\sim 24$  hours) is only a fraction of the cost of a direct multi-objective optimization being well over few thousands (estimated based on the number of  $R_s$  evaluations during MOEA-based Pareto set identification).

## 4 Conclusions

In this work, a technique for design space reduction in the context of multi-objective optimization of antenna structures using variable-fidelity EM simulations and RSA-based surrogate is presented. A fast generation of a reliable RSA model is possible even for larger number of designable parameters of the antenna of interest. The proposed method is validated using a UWB monocone, and a planar Yagi-Uda antenna. The Pareto optimal set is obtained at a cost of a few dozen of high-fidelity EM antenna simulations, which is a significant speedup compared to direct multi-objective optimization of the high-fidelity antenna model.

## References

- Afshinmanesh, F., Marandi, A., Shahabadi, M. (2008) *Design of a Single-Feed Dual-Band Dual-Polarized Printed Microstrip Antenna Using a Boolean Particle Swarm Optimization*. IEEE Trans. Antennas Prop., 56, 1845-1852.
- Bandler, J.W., Cheng, Q.S., Dakrouy, S.A., Mohamed, A.S., Bakr, M.H., Madsen, K., Søndergaard, J. (2004) *Space mapping: the state of the art*. IEEE Trans. Microwave Theory Tech., 52, 337-361.
- Beachkofski, B., Grandhi, R. (2002) *Improved distributed hypercube sampling*. American Institute of Aeronautics and Astronautics. Paper AIAA 2002—1274.
- Cao, W., Zhang, B., Liu, A., Yu, T., Guo, D., Wei, Y. (2012) *Broadband High-Gain Periodic Endfire Antenna by Using I-Shaped Resonator (ISR) Structures*. IEEE Antennas Wireless Prop. Lett., 11, 1470-1473.
- CST Microwave Studio (2013). Computer Simulation Technology AG, Bad Nauheimer Str. 19, D-64289 Darmstadt, Germany.
- Deb, K. (2001) *Multi-Objective Optimization Using Evolutionary Algorithms*. John Wiley & Sons.
- Ding, D., Wang, G. (2013) *Modified Multiobjective Evolutionary Algorithm Based on Decomposition for Antenna Design*. IEEE Trans. Antennas Prop., 61, 5301-5307.
- Eichfelder, G. (2008) *Adaptive Scalarization Methods in Multiobjective Optimization*. SIAM Journal on Opt., 19, 1694-1718.
- Hannien, I. (2012) *Optimization of a Reflector Antenna System*. Computer Simulation Technology AG whitepaper, 1-4.
- Jin, N., Rahmat-Samii, Y. (2010) *Hybrid Real-Binary Particle Swarm Optimization (HPSO) in Engineering Electromagnetics*. IEEE Trans. Antennas Prop., 58, 3786-3794.
- Jungsuek, O., Sarabandi, K. (2013) *A Topology-Based Miniaturization of Circularly Polarized Patch Antennas*. IEEE Trans. Antennas Prop., 61, 1422-1426.
- Kolda, T.G., Lewis, R.M., Torczon, V. (2003) *Optimization by direct search: new perspectives on some classical and modern methods*. SIAM Review, 45, 385-482.
- Koulouridis, S., Psychoudakis, D., Volakis, J. (2007) *Multiobjective Optimal Antenna Design Based on Volumetric Material Optimization*. IEEE Trans. Antennas Prop., 55, 594-603.



- Koziel, S., Ogurtsov, S. (2011) *Rapid design optimization of antennas using space mapping and response surface approximation models*. Int. J. RF & Microwave CAE, 21, 611-621.
- Koziel, S., Ogurtsov, S. (2013) *Multi-Objective Design of Antennas Using Variable-Fidelity Simulations and Surrogate Models*. IEEE Trans. Antennas Prop., 61, 5931-5939.
- Koziel, S., Cheng, Q.S., Bandler, J.W. (2008) *Space mapping*. IEEE Microwave Magazine, 9, 105-122.
- Koziel, S., Ogurtsov, S., Szczepanski, S. (2012) *Rapid antenna design optimization using shape-preserving response prediction*. Bulletin of the Polish Academy of Sciences. Technical Sciences, 60, 143-149.
- Koziel, S., Leifsson, L., Ogurtsov, S. (2013) *Reliable EM-driven microwave design optimization using manifold mapping and adjoint sensitivity*. Microwave Opt. Tech. Lett., 55, 809-813.
- Kuwahara, Y. (2005) *Multiobjective optimization design of Yagi-Uda antenna*. IEEE Trans. Antennas Prop., 53, 1984-1992.
- Lophaven, S.N., Nielsen, H.B., Søndergaard, J. (2002) *DACE: a Matlab kriging toolbox*. Technical University of Denmark.
- Nair D., Webb, J.P. (2003) *Optimization of microwave devices using 3-D finite elements and the design sensitivity of the frequency response*. IEEE Trans. Magnetics, 39, 1325-1328.
- Qian, Y., Deal, W.R., Kaneda, N., Itoh, T. (1998) *Microstrip-fed quasi-Yagi antenna with broadband characteristics*. Electronics Letters, 34, 2194-2196.
- Sharaqa, A., Dib, N. (2013) *Position-only side lobe reduction of a uniformly excited elliptical antenna array using evolutionary algorithms*. IET Microwaves, Antennas Prop., 7, 452-457.
- Simpson, T.W., Peplinski, J., Koch, P.N., Allen, J.K., (2001) *Metamodels for computer-based engineering design: survey and recommendations*. Engineering with Computers, 17, 129-150.
- Yang, X.-S., Ng, K.-T., Yeung, S.H., Man, K.F. (2008) *Jumping Genes Multiobjective Optimization Scheme for Planar Monopole Ultrawideband Antenna*. IEEE Trans. Antennas Prop., 56, 3659-3666.